Supporting information for:

Nearly Monodisperse Insulator Cs_4PbX_6 (X = Cl, Br, I) Nanocrystals, Their Mixed Halide Compositions, and Their Transformation into $CsPbX_3$ Nanocrystals

Quinten A. Akkerman,[†,φ,Δ] Sungwook Park,[†,§,Δ] Eros Radicchi,[⊥,‖] Francesca Nunzi,[⊥,‖] Edoardo Mosconi,[‖,#] Filippo De Angelis,[‖,#] Rosaria Brescia[†], Prachi Rastogi,[†,φ] Mirko Prato[†,*] and Liberato Manna[†,*]

[†]Nanochemistry Department, Istituto Italiano di Tecnologia, Via Morego 30, 16163 Genova, Italy

[φ]Università degli Studi di Genova, Via Dodecaneso, 31, 16146, Genova, Italy

[§]Department of Physics, Pukyong National University, Busan 608-737, Korea

[⊥]Computational Laboratory of Hybrid/Organic Photovoltaics (CLHYO), CNR-ISTM, via Elce di Sotto 8, I-06123 Perugia, Italy.

[‖]Dipartimento di Chimica, Biologia e Biotecnologie, Università degli Studi di Perugia, via Elce di Sotto 8, I-06123 Perugia, Italy.

[#]CompuNet, Istituto Italiano di Tecnologia, Via Morego 30, 16163 Genova, Italy.

*These authors contributed equally to this work

EXPERIMENTAL DETAILS

Chemicals. Lead(II) chloride ($PbCl_2$, 99.999% trace metals basis), lead(II) bromide ($PbBr_2$, 99.999% trace metals basis), lead(II) iodide (PbI_2, 99.999% trace metals basis), cesium carbonate (Cs_2CO_3, reagentPlus, 99%), n-hexane (HEX, 99.5%), isopropyl alcohol (IPrOH, ≥99.7%), acetonitrile (AcN, anhydrous, 99.8%), octadecene (ODE, technical grade, 90%), oleylamine (OLAM, 70%) and oleic acid (OA, 90%) were purchased from Sigma-Aldrich. Toluene (TOL, anhydrous, 99.8%) was purchased from Carlo Erba reagents. All chemicals were used without any further purification.

Cs_4PbX_6 NCs synthesis and purification. All syntheses were performed in air and without any pre-dried chemicals or solvents. In a typical synthesis, PbX_2 (0.1 mmol) was dissolved in 5 mL ODE, 0.2 mL OA and 1.5 mL OLAM in a 20 mL vial on a hotplate set at 150 °C. After the PbX_2 was completely dissolved (around 100 ^{0}C), the vial was moved to a room temperature (RT) hotplate, and the solution was allowed to cool. When the temperature reached the optimal value (80 ^{0}C for $PbBr_2$, 100 ^{0}C for $PbCl_2$ or 60 ^{0}C for PbI_2), 0.75 mL of Cs-OA (0.4 g Cs_2CO_3 dissolved in 8 mL OA in a 20 ml vial on a hotplate set to 150 ^{0}C) was swiftly injected. After about 30 seconds the reaction turned turbid white and, depending on the required size, was quickly cooled down after 0-10 min to RT with a cold water bath. The NCs were directly washed *via* centrifugation (at 4500 rpm for 10 minutes), followed by redispersion in 6 ml TOL (or HEX for optical measurements).

$Cs_4Pb(Br:X)_6$ (X = Cl, I) NCs synthesis and purification via inter-particle anion-exchange. All inter-particle anion-exchange were performed in air and without any pre-dried chemicals or solvents similar to our previous report. In a typical exchange, equal volumetric amounts (from the purified NC solutions as described above) of Cs_4PbBr_6 and Cs_4PbI_6 or Cs_4PbCl_6 and were left stirring overnight at room temperature. The NCs were not further purified.

Reaction of Cs_4PbBr_6 NCs with $PbBr_2$ to yield $CsPbBr_3$ NCs and their purification. All syntheses were performed in air and without any pre-dried chemicals or solvents. In a typical reaction, 0.5 ml of Cs_4PbBr_6 NC solution was diluted in 2 ml of TOL and heated on a hotplate set at 80 °C. After the temperature was stable, 50 µl of $PbBr_2$ precursor was injected (1 mmol $PbBr_2$ dissolved in 0.5 mL TOL, 0.25 mL OA and 0.25 mL OLA). Within 1 minute, the solution

started turning green and after 15-60 minutes, depending on the size of the Cs_4PbBr_6 NCs, the reaction was cooled down to RT with a cold water bath. The NCs were directly washed by centrifugation (at 4500 rpm for 10 minutes), followed by redispersion in TOL.

Transmission Electron Microscopy (TEM). Conventional TEM images were acquired on a JEOL JEM-1011 microscope equipped with a thermionic gun at 100 kV accelerating voltage. High-resolution TEM (HRTEM) imaging was performed on a JEOL JEM-2200FS microscope equipped with a Schottky gun operated at 200 kV accelerating voltage, a CEOS spherical aberration corrector in objective lens enabling a spatial resolution of 0.9 Å, and an in column image filter (Ω-type). The samples were prepared by drop casting diluted NC suspensions onto 200 mesh carbon-coated copper grids for conventional TEM imaging, and 400 mesh ultrathin/holey carbon-coated copper grids for HRTEM imaging, respectively. **Powder X-ray Diffraction (XRD) Analysis.** XRD patterns were obtained using a PANalytical Empyrean X-ray diffractometer equipped with a 1.8 kW Cu Kα ceramic X-ray tube, PIXcel3D 2x2 area detector and operating at 45 kV and 40 mA. The diffraction patterns were collected in air at room temperature using Parallel-Beam (PB) geometry and symmetric reflection mode. All XRD samples were prepared by drop casting a concentrated solution on a zero diffraction silicon wafer.

Inductively Coupled Plasma Optical Emission Spectroscopy (ICP-OES). ICP-OES analysis performed on an iCAP 6000 spectrometer (ThermoScientific) was used to quantify the Pb content in the solutions of $CsPbBr_3$ and Cs_4PbBr_6 NCs. Prior to measurements, the samples were decomposed in aqua regia (HCl/HNO3 = 3/1 (v/v)) overnight.

Optical Absorption Spectroscopy. The spectra were taken on a Varian Cary 5000 UV−vis−NIR spectrophotometer. Samples were prepared by diluting the NC solutions in hexane or toluene in 1 cm path length quartz cuvettes.

Photoluminescence (PL) and Photoluminescence Quantum Yield (PLQY) measurements. The PL spectra were taken on a Varian Cary Eclipse spectrophotometer. Samples were prepared by diluting the various NC solutions in toluene, in quartz cuvettes with a path length of 1 cm. PLQY measurements were carried out in solutions with an Edinburgh Instruments fluorescence spectrometer (FLS920), which included a xenon lamp with monochromator for steady-state PL excitation. A calibrated integrating sphere was used for PLQY measurements. The nanocrystals/perovskite NCs solutions in toluene were prepared in quartz cuvettes and diluted to 0.1 optical density at the excitation wavelength 400 nm.

Density functional theory (DFT) calculations. The Amsterdam Density Functional program package (ADF2014)[1-3] has been used for all the calculations. Starting from the experimental molecular geometries of Cs_4PbX_6 NCs (X= Br, I), we carried out DFT single point (SP) energy calculations in the gas phase on selected NC clusters, modelling the various feasible mixed halide composition. In particular, we resort to the B3LYP exchange-correlation functional (including the Vosko-Wilk-Nusair LDA parametrization and 20% of Hartree-Fock exchange), together with a Slater type TZP basis set for all the atoms (the cores 1s-2p, 1s-3p, 1s-4p and 1s-4d were kept frozen, respectively for Cl, Br, I and Pb) and a ZORA Hamiltonian to include relativistic effects. We employed either the scalar and the spin-orbit (SO) ZORA Hamiltonian, the latter used in order to consider spin orbit coupling (SOC) effects. Time Dependent (TD) DFT calculations have been performed using the B3LYP exchange-correlation functional. The relativistic TDDFT formalism as implemented in ADF for closed-shell molecules, including SOC, is based on the ZORA two components Hamiltonian.[4-5] Relativistic spectra have been evaluated taking into account the SOC in a self-consistent perturbative way.[6] The 12 lowest transitions have been considered in each case. The absorption spectra have been simulated by interpolating the computed transitions by Gaussian functions with a broadening σ=0.075, corresponding to an FWHM of 0.18 eV, thus matching the experimental one. The TDDFT calculations are carried out on negatively-charged $[PbX_6]^{4-}$ clusters, where the caesium cations are replaced by including in the Fock operator an electric field due to point charges, fixed in the octahedral corners and formally equivalent to an overall charge of +4. The Pb-X distances are taken from the corresponding 3D perovskite at 3.164 and 2.950 Å for X=I and Br, respectively. The accuracy of the model in reproducing the main electronic features has been validated through comparative calculations on both the neutral Cs_4PbX_6 NC and the PbX_6^{4-} anion at the same level of theory showing a variation of the calculated HOMO-LUMO gap within less than 0.2 eV. Periodic Boundary Conditions DFT calculations were performed on the Cs_4PbBr_6 crystal at its experimental geometry and cell parameters, using the

QuantumEspresso simulation package.[7] PBE calculations have been performed by using ultrasoft pseudopotentials with a cutoff on the wavefunction of 25 Ry (200 Ry on the charge density) and uniform grid of k-points in the Brillouin Zone.[8]

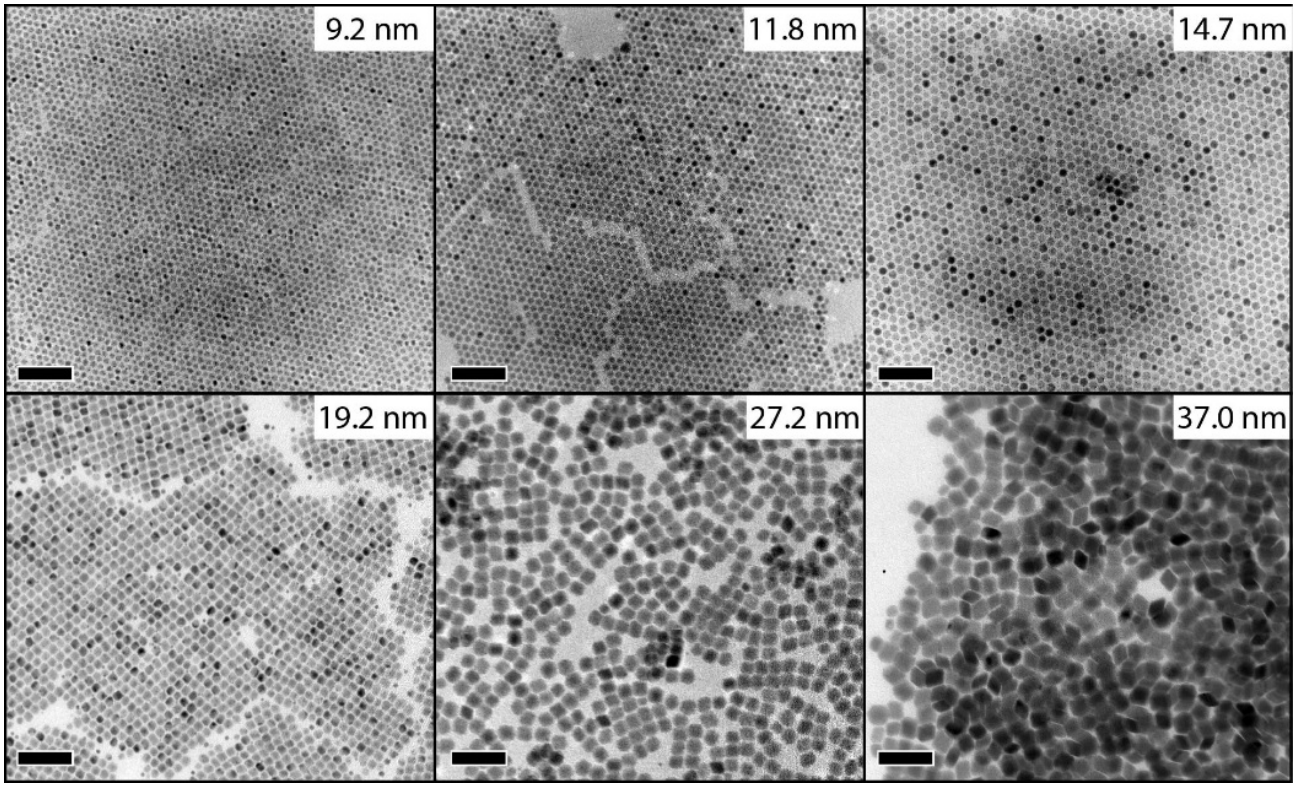

Figure S1. Different sized Cs_4PbBr_6 NCs. Scale bars correspond to 100 nm.

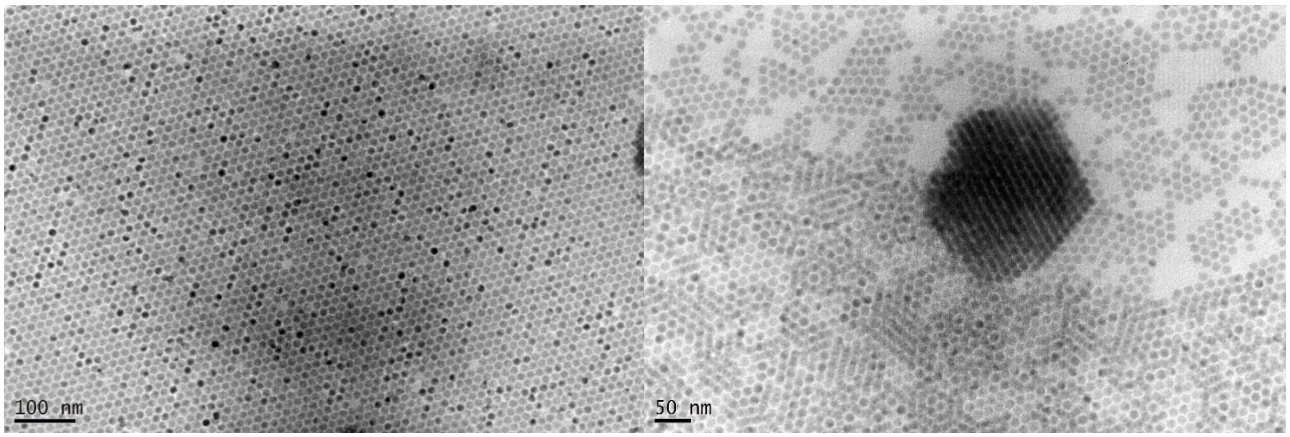

Figure S2. (left) Large area of Cs_4PbBr_6 NCs. (right) Large self-assembled cluster for Cs_4PbBr_6.

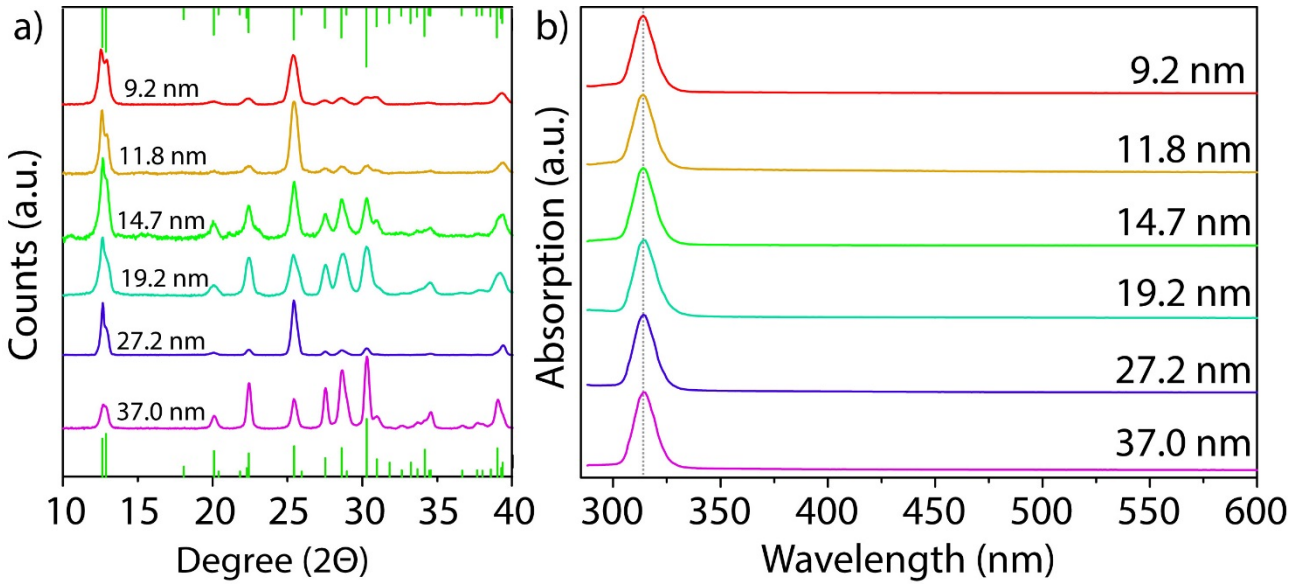

Figure S3. (a) Diffraction patterns of different sized Cs_4PbBr_6 NCs. (b) Absorption of different sized Cs_4PbBr_6 NCs. Cs_4PbBr_6 reference pattern 98-002-5124.

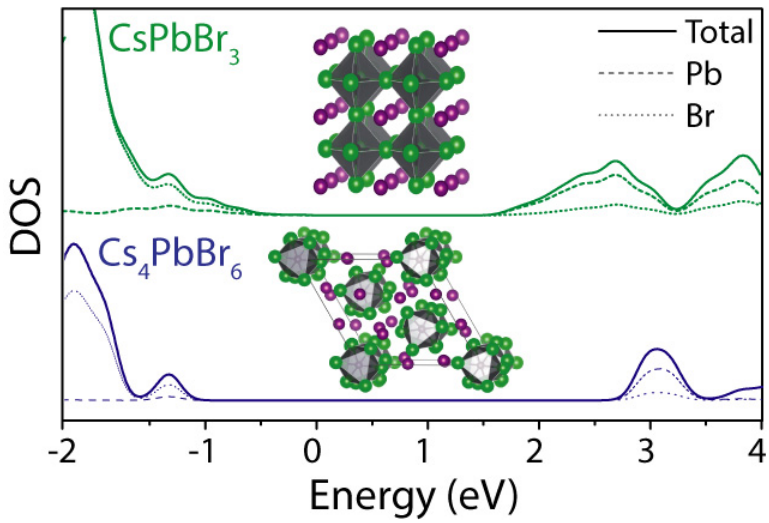

Figure S4. Density of states calculations for $CsPbBr_3$ and Cs_4PbBr_6.

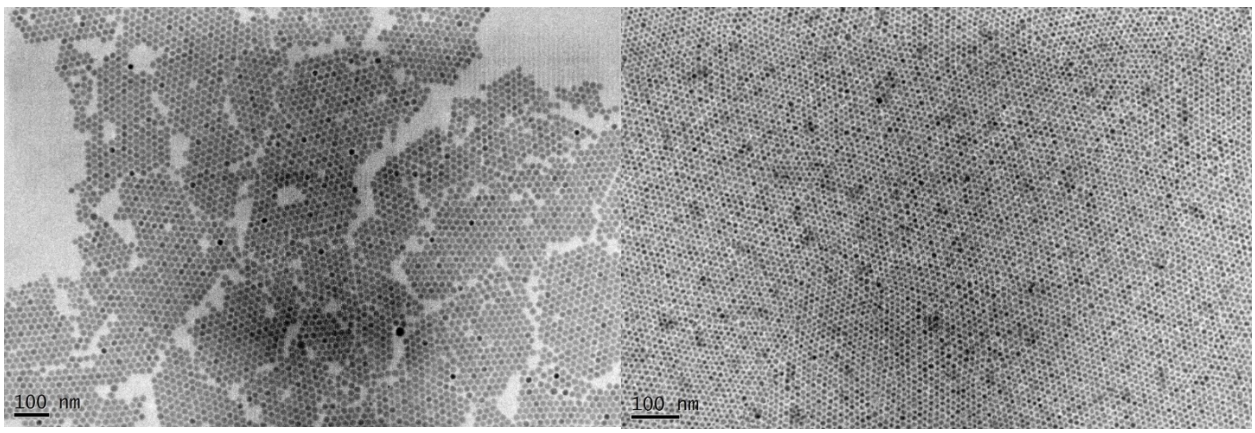

Figure S5. (left) Large area TEM images of Cs_4PbCl_6 NCs (left) and Cs_4PbI_6 NCs (right).

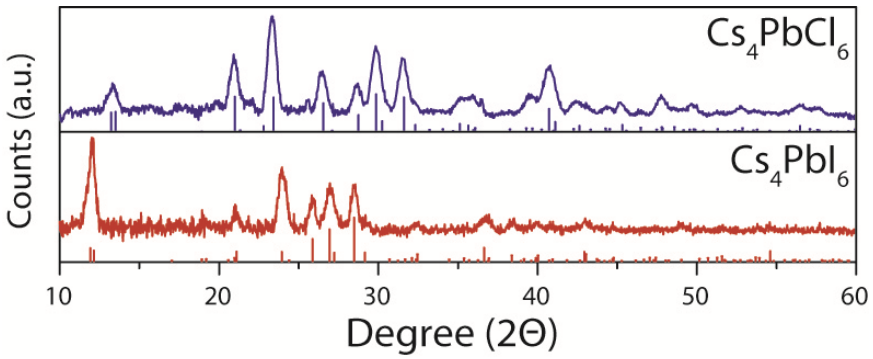

Figure S6. XRD patterns for Cs_4PbCl_6 NCs (top) and Cs_4PbI_6 NCs (bottom). XRD references cards 98-002-5123 for Cs_4PbCl_6 and 1602013 for Cs_4PbI_6.

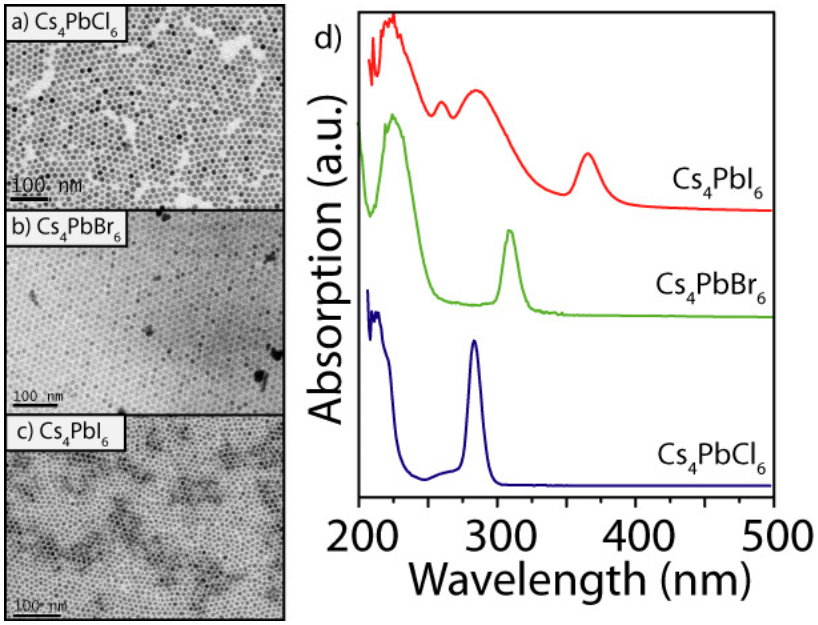

Figure S7. TEM images of (a) Cs_4PbCl_6, (b) Cs_4PbBr_6 and (c) Cs_4PbI_6 NCs stored for one month under ambient conditions. (d) Absorption spectra indicated no degradation of NCs.

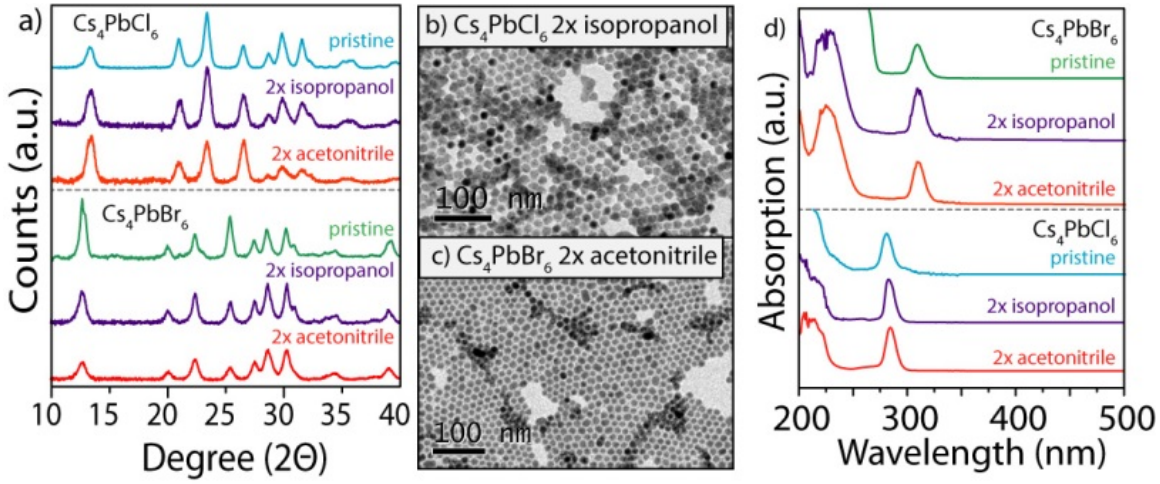

Figure S8. (a) XRD patterns for Cs_4PbCl_6 NCs and Cs_4PbBr_6 NCs after washing twice with isopropanol and acetonitrile. TEM images of (b) Cs_4PbCl_6 NCs and (c) Cs_4PbPb_6 NCs after washing. (d) The optical absorption spectra indicated no degradation of NCs after washing with polar solvents.

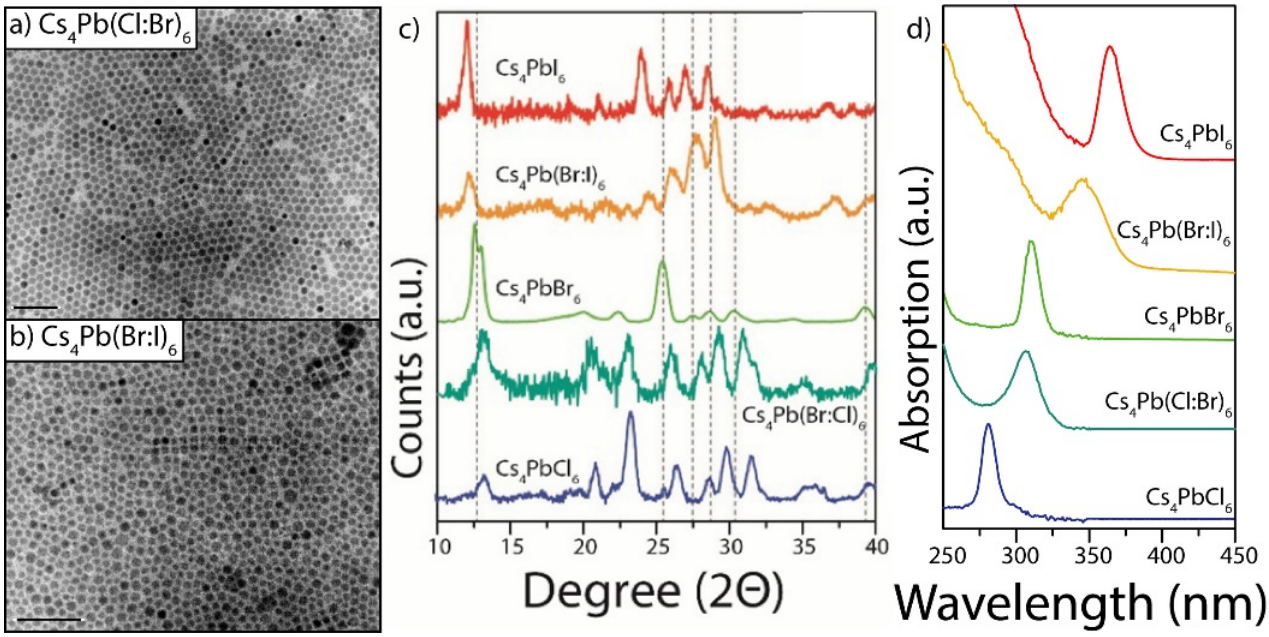

Figure S9. TEM images of (a) $Cs_4Pb(Cl:Br)_6$ NCs and (b) $Cs_4Pb(Br:I)_6$ NCs obtained via direct synthesis. (c) XRD patterns prove the mixed halide Cs_4PbBr_6 NCs and confirm intermediate lattice parameters compared to the pure phases. (d) Optical absorption spectra of the mixed halide NCs and the pristine NCs. Scale bars in (a) and (b) correspond to 100 nm.

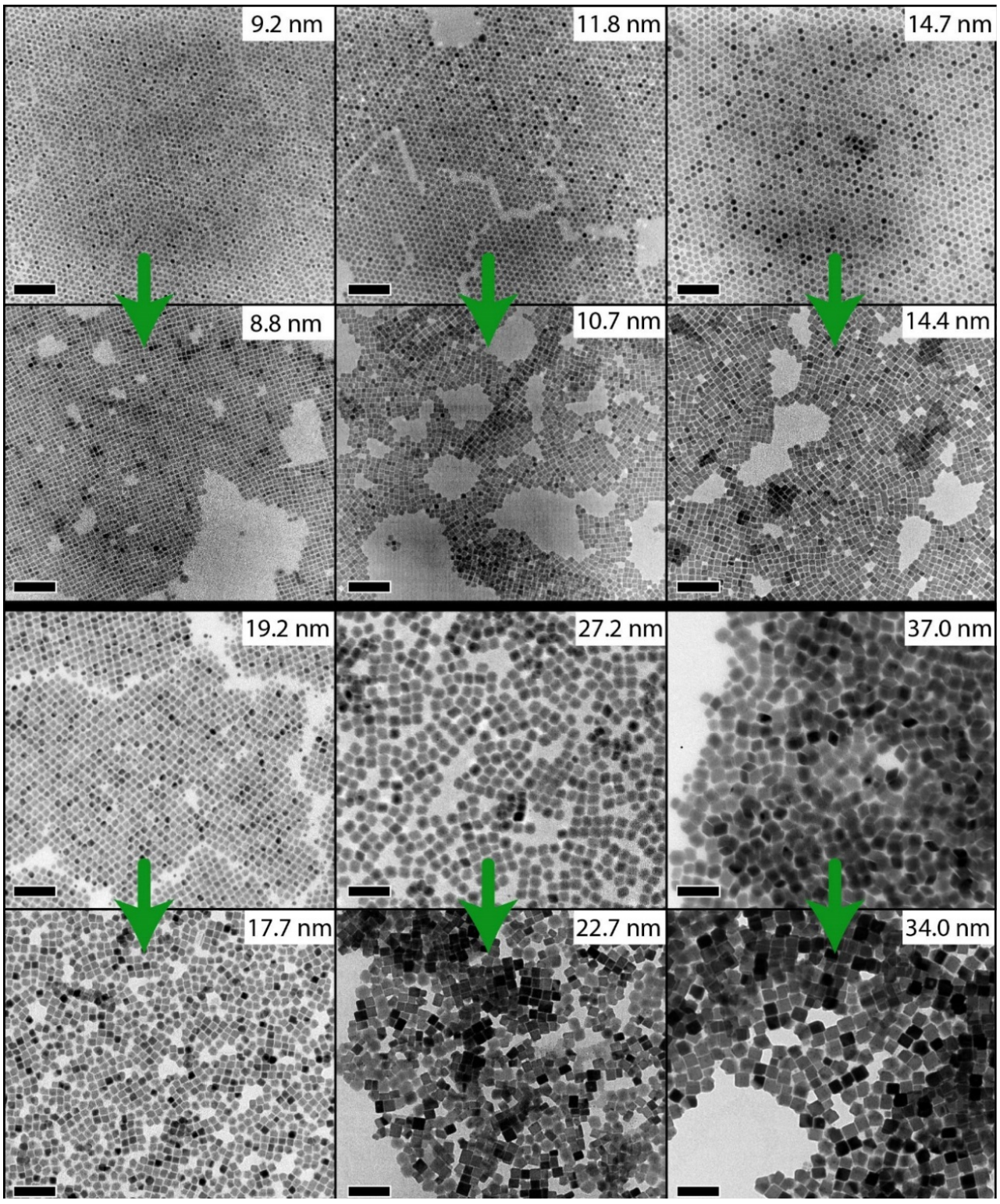

Figure S10. Overview of $CsPbBr_3$ NCs obtained via insertion reaction of $PbBr_2$ on Cs_4PbBr_6. All scale bars correspond to 100 nm.

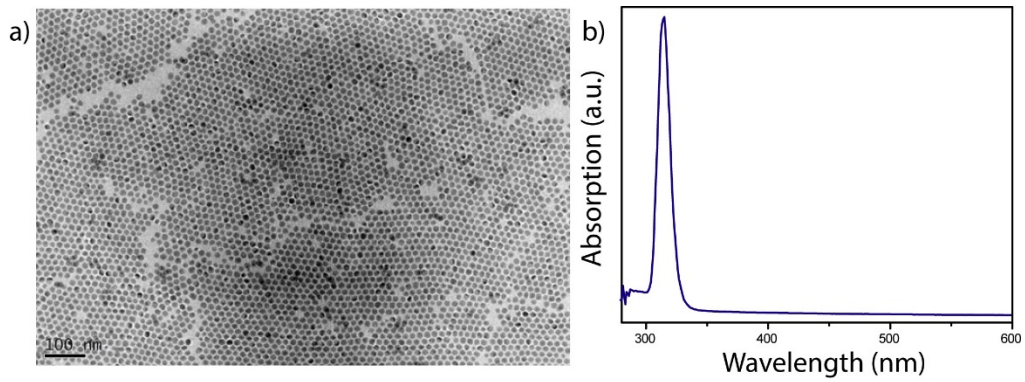

Figure S11. (a) TEM image and (b) absorption of Cs_4PbBr_6 NCs after (45 min) insertion reaction, without the addition of $PbBr_2$.

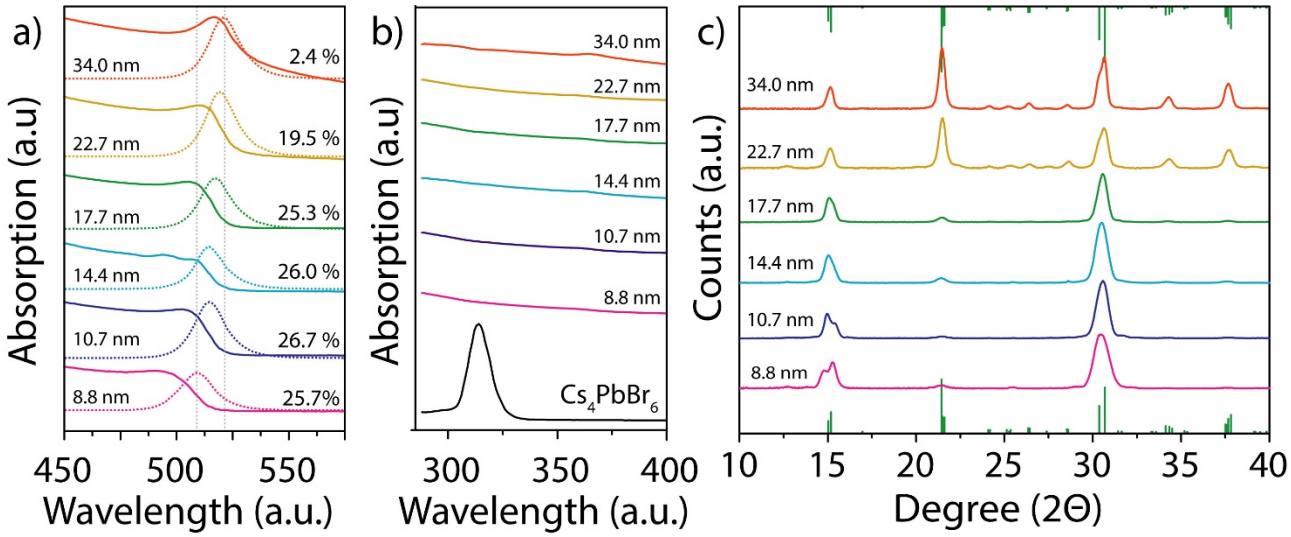

Figure S12. (a) Photoluminescence and PLQY, (b) absorption and (c) XRD data of different sized $CsPbBr_3$ NCs obtained via insertion reaction with $PbBr_2$. $CsPbBr_3$ XRD reference pattern 98-002-5124.

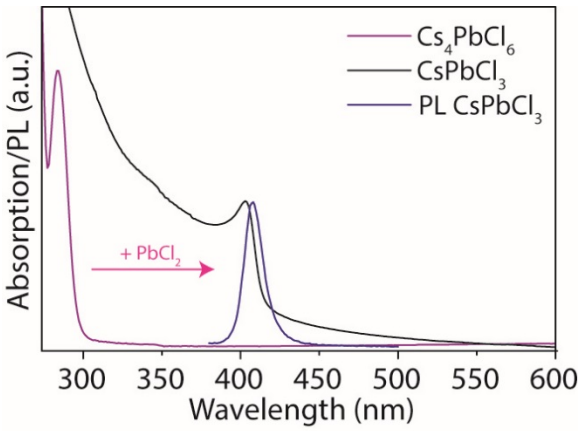

Figure S13. Optical absorption of Cs_4PbCl_6 NCs (magenta) and optical absorption (black) and PL (blue) spectra of the $CsPbCl_3$ NCs obtained from them by reaction with $PbCl_2$. The absorption tail for the $CsPbCl_3$ NCs at longer wavelengths is most likely due to aggregation effects.

References

(1) te Velde, G.; Bickelhaupt, F. M.; Baerends, E. J.; Guerra, C. F.; Van Gisbergen, S. J. A.; Snijders, J. G.; Ziegler, T., *J. Comput. Chem.* **2001**, *22*, 931-967.
(2) Guerra, C. F.; Snijders, J. G.; te Velde, G.; Baerends, E. J., *Theor. Chem. Acc.* **1998**, *99*, 391-403.
(3) Walsh, A., *J. Phys. Chem. C* **2015**, *119*, 5755-5760.
(4) Visscher, L.; van Lenthe, E., *Chem. Phys. Lett.* **1999**, *306*, 357-365.
(5) Vanlenthe, E.; Baerends, E. J.; Snijders, J. G., *J. Chem. Phys.* **1993**, *99*, 4597-4610.
(6) Wang, F.; Ziegler, T., *J. Chem. Phys.* **2005**, *123.*
(7) P. Giannozzi et al., QUANTUM ESPRESSO: a modular and open-source software project for quantum simulations of materials. *J. Phys. Condens. Matter.* 21, 395502 (2009).
(8) J. P. Perdew, K. Burke, M. Ernzerhof, Generalized Gradient Approximation Made Simple. *Phys. Rev. Lett.* 77, 3865–3868 (1996)